Relaxation of Stretched DNA in Slitlike Confinement

A. Balducci, C.-C. Hsieh, and P. S. Doyle*

Massachusetts Institute of Technology, Cambridge, Massachusetts 02139, USA

(Received 24 July 2007; published 6 December 2007)

We experimentally observe two separate time scales governing the entropic recoil in the linear force-extension regime of single double-stranded DNA in slit confinement. We demonstrate the existence of two distinct relaxation regimes at different extensions during relaxation. Contrary to bulk measurements, the true longest relaxation time may only be probed very close to equilibrium. A simple model of the relaxation mechanism leads to a scaling analysis that correctly predicts the extension at the crossover between the two regimes.

DOI: 10.1103/PhysRevLett.99.238102 PACS numbers: 87.15.He, 82.37.Rs, 87.14.Gg

Micro- and nanofluidic systems show much promise in their ability to precisely control flows, reactions, and even biological separations [1]. Microdevices have recently been used in DNA separations [2] and single-molecule mapping [3]. The performance of such devices is highly dependent on the conformation of the polymer in response to collisions [4] and field gradients [3]. The deformation of the polymer is the result of a competition between the imposed stretching rate and polymer relaxation. Therefore, to efficiently design new devices, it is important to understand the effects of confinement on the relaxation of a polymer.

Historically, blob theory has been used as a method to study slit-confinement effects on the longest relaxation time of a polymer [5]. Several studies have since characterized the relaxation time of DNA in slit confinement. An experimental study by Bakajin *et al.* [6] presented the relaxation of initially stretched DNA as a function of time. The authors reported that the longest relaxation time increased with decreasing channel height, as expected. A later study [7], in an effort to compare new longest relaxation time results obtained through conformational fluctuations at equilibrium, fit the data from Bakajin *et al.* to a single-exponential decay over available extensions (~50% to 10%). Results from the two studies give different apparent longest relaxation times [7]. Furthermore, each experimental study is supported by analogous computer simulations. Simulations of a relaxing chain with hydrodynamic interactions (HI) have been able to reproduce the extension data of Bakajin *et al.* [8,9] but were not compared to blob theory. Monte Carlo simulations, which access the relaxation time through fluctuations at equilibrium but neglect HI, have found scalings in accord with a free-draining blob theory [10,11]. These Monte Carlo results are in better agreement with the more recent experimental findings [7]. Taken together, these previous results suggest that different relaxation modes may be probed in the recoil and equilibrium studies.

In this Letter, we argue that slit confinement induces a new relaxation regime. Experimental results of the extension evolution of a confined, relaxing chain are best described by *two* distinct time constants within the linear force-extension regime. In contrast, experiments on unconfined DNA show that a single time constant describes the dynamics of a relaxing chain from the onset of the linear force regime (~30% extension) to equilibrium [12,13]. We show that a simple scaling analysis correctly predicts the crossover between the two regimes as well as relaxation time scalings near equilibrium. We also show that, in slit confinement, the true longest relaxation time governs the dynamics of the polymer only very close to equilibrium and thus can be easily overlooked without careful analysis.

The relaxation of T4 DNA (165.6 kbp, Nippon Gene) and λ-DNA concatamers (194, 242.5, and 291 kbp, referred to as 4λ-, 5λ-, and 6λ-DNA, respectively) were observed in a 1 μm tall glass microchannel unless otherwise noted (Fig. 1). λ-DNA (New England Biolabs, NEB) was ligated with T4 ligase (NEB) for 25 minutes. All DNA samples were stained with YOYO-1 (Invitrogen) dye at 4 bp per dye molecule and diluted into 0.5× TBE (Omnipur) which contained 4% (vol.) beta-mercaptoethanol (Cabiochem), 12.5 mg/mL glucose (Mallinckrodt), 0.16 mg/mL glucose oxidase (Roche), 7.4 μg/mL catalase (Roche), and 0.1% (wt.) 10 kDa poly(vinylpyrrolidone) (Polysciences). The 200 μm wide microchannel contained three rows of 2 μm diameter cylindrical obstacles spaced at 4 μm. An electric field was used to stretch the DNA on the obstacles and was turned off after the stretched DNA exited the post array. The λ-DNA concatamers were identified during a symmetric collision by measuring the contour length (L_c) of the nearly fully extended molecule. Our imaging setup and image analysis is described elsewhere [7,14]. The extension (X_{ex}) was determined by the projected distance along the initial stretch direction.

Figure 2(a) displays the scaled squared extension of the DNA as a function of time for increasing molecular weight. Each curve represents the ensemble average of 20–45 molecules. Previous work has explained the need to fit the squared extension in single-molecule relaxation experi-

ments in order to extract a longest relaxation time that agrees with rheological measurements [13]. The curves in Fig. 2(a) display two distinct time constants: one near 30% extension and another near equilibrium. A different presentation of the data for 4λ-DNA is shown in the inset where the decay has been normalized such that the plot should be horizontal over the region in which the fitted time constant describes the decay. The inset figure shows two time-distinct plateaus, and each fitted region persists in time for more than twice the applicable time constant. The crossover (taken as the intersection of the extrapolated fits) occurs at a relatively constant scaled square extension of 0.002 to 0.005 or relative extensions (X_{ex}/L_c) of 7 to 9%. In this Letter, the higher extension time constant will be referred to as τ_I and the low-extension time constant as τ_{II}. Table I displays both relaxation times, and Fig. 2(b) shows the results of this study in comparison to previous results in slit confinement [6,7]. We propose that the two different relaxation time constants found in this study are due to two different relaxation mechanisms present at different extensions and not due to the nonlinear elasticity of the DNA.

Although we study extensions in the linear force regime, there may be several reasons for the observed change in slope in Fig. 2(a). For example, when the stretched DNA leaves the obstacle the tension distribution is initially asymmetric. To check this, we calculate the distance from the right and left end points of the chain to the center of mass as a function of time and fit our data only after the relaxation is symmetric around the center of mass [14]. Symmetry is obtained very shortly after the DNA leaves the post (1–2 s), suggesting that the asymmetric tension distribution quickly reequilibrates throughout the chain [15]. Further, an accurate measure of the mean equilibrium extension ($\langle X_{ex,eq}\rangle$) is needed in order for the data in Fig. 2(a) to properly decay to zero at long times. We investigated both the polymer size and diffusivity at equilibrium [Fig. 3(a)] and find these are in agreement with blob theory [16,17], confirming that the polymers are confined at equilibrium. To ensure this transition is truly caused by confinement effects, we qualitatively compare the relaxation of T4 DNA in a 1 and 2 μm tall channel [Fig. 3(b)]. If the transition is caused by confinement, we expect to delay or completely eliminate the transition by increasing the channel height. The transition is absent in the 2 μm channel. We will return to this result. We conclude that the existence of two separate relaxation regimes is indeed a confinement effect.

To explain the scalings of these relaxation regimes as well as the crossover point between them, we utilize a simple scaling model of the recoil. We describe the polymer in a tension-blob framework until the dimension of the tension blob is equivalent to the height of the channel. At this point, the confining effects of the channel walls become important (see Fig. 1). Before this point, relaxation occurs by increasing the size of the tension blobs along the chain, as if it were in bulk but with a modified drag coefficient. After this point, the blobs can no longer grow and must rearrange within the channel to further dissipate stress. The second regime is equivalent to the relaxation of a quasi-two-dimensional self-avoiding chain.

If we take the relaxation to be quasisteady, good solvent scalings within blobs, and minimal rotation of the molecule during the initial relaxation, then the crossover between the two above mechanisms occurs when blobs that span the height of the channel are perfectly aligned in the direction of original stretch. Using this criterion, the relative extension at the crossover point is

$$\frac{X_{ex}}{L_c} = \frac{hN_{blobs}}{Nb} = 2^{5/3} a_{bulk}^{5/3} b^{1/3} h^{-2/3}, \quad (1)$$

where h is the height of the channel, and a_{bulk} is the proportionality constant relating the bulk radius of gyration ($R_{g,bulk}$) to the number of Kuhn steps ($N = L_c/b$):

$$R_{g,bulk} = a_{bulk} b^{4/5} N^{3/5}. \quad (2)$$

Note that a_{bulk} incorporates an effective excluded volume diameter. Using $R_{g,bulk} = 0.69$ μm [7], $L_c = 21.5$ μm, and $b = 106$ nm for stained λ-DNA, we find $a_{bulk} = 0.17$ μm$^{1/5}$. Equation (1) predicts a crossover extension of 8.0% [0.003 to 0.004 on the ordinate of Fig. 2(a)], in very good agreement with the experimental results. The crossover extension is not dependent on molecular weight, but depends on channel height and solvent quality, ionic strength, and temperature through dependencies in b and a_{bulk}. We can confirm the assumption of negligible rotation by measuring the average angle between the principle axis of the DNA and the original stretch direction [Fig. 3(c)]. The DNA tend to stay oriented in the direction of original

TABLE I. Relaxation times in a 1 μm tall channel.

	T4 DNA	4λ-DNA	5λ-DNA	6λ-DNA
τ_I (s)	2.1 ± 0.1	3.5 ± 0.1	4.9 ± 0.2	7.4 ± 0.3
τ_{II} (s)	3.7 ± 0.7	5.8 ± 0.8	9.0 ± 2.6	13.5 ± 2.2

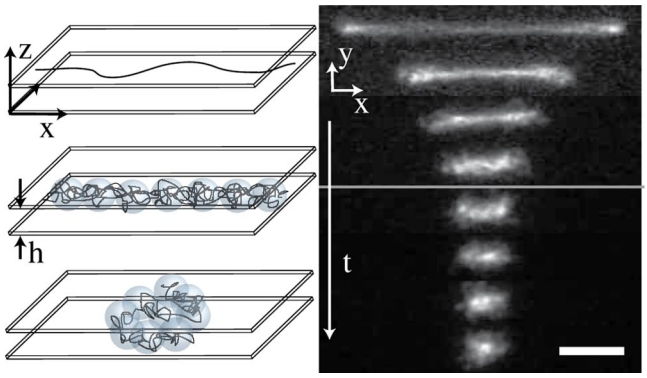

FIG. 1 (color online). Schematic of confined polymer relaxation along with ensemble-averaged time-series images of 5λ-DNA. The time between the images is 5 s and the scale bar is 10 μm. The gray line represents the predicted crossover between the two relaxation regimes discussed in this Letter.

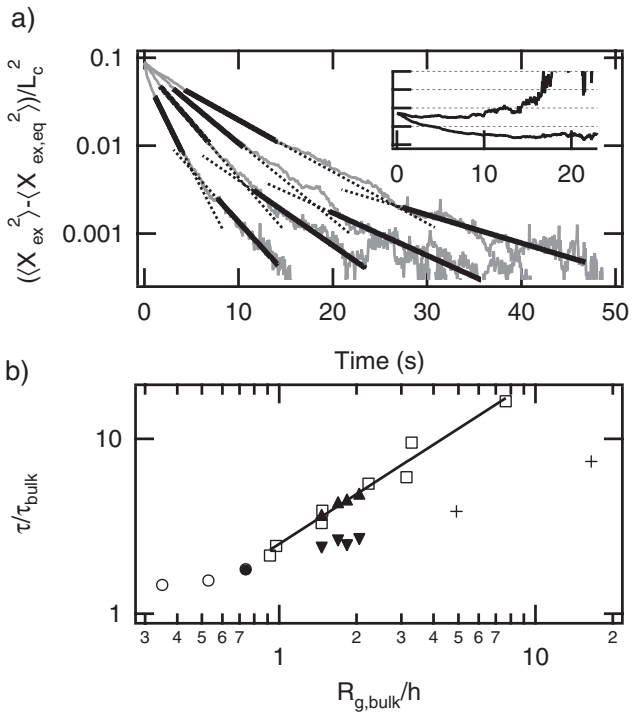

FIG. 2. (a) Normalized extension vs time (t) for T4, 4λ-, 5λ-, and 6λ-DNA from left to right. $X_{ex}/L_c = 0.3$ at $t = 0$. Solid lines are fits to the data; dotted lines are extrapolations of the fits to guide the eye. Regime I is fit to a single exponential from the onset of symmetric relaxation (see text) until approximately twice the crossover extension predicted by Eq. (1). Regime II is fit from half the crossover extension to statistical noise taken as the equilibrium extension ($X_{ex,eq}$, a typical fluctuation distance) divided by the square root of the number of DNA molecules observed. Inset: $(\langle X_{ex}^2\rangle - \langle X_{ex,eq}^2\rangle)/[L_c^2 \exp(-t/\tau_n)]$, n = I, II for 4λ-DNA vs time in seconds. (b) Measured relaxation time in confinement normalized by bulk relaxation time vs the inverse channel height normalized by the bulk radius of gyration. Open symbols are previous measurements by our group [7], + are single-exponential fits [7] to data from Bakajin *et. al.* [6], and data from this study are represented by ▼(τ_I), ▲ (τ_{II}), and ● (T4 DNA, $h = 2$ μm). The solid line is an empirical fit from Ref. [7] with slope 0.92.

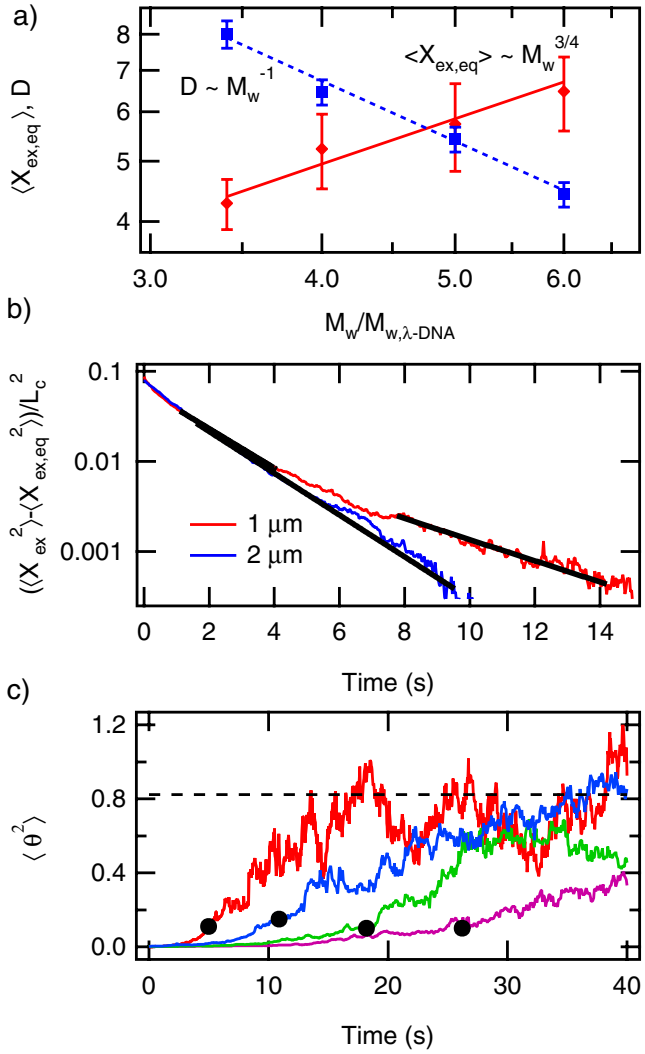

FIG. 3 (color online). (a) Equilibrium extension (μm) and diffusion coefficient (10^2 $\mu m^2/s$) vs molecular weight normalized by that of λ-DNA. Lines are scaling predictions from blob theory. (b) Scaled squared extension of T4 DNA recoil in a 1 and 2 μm tall channel. Solid black lines are fits to the data. (c) Angle between the DNA principle axis and the original stretch direction for increasing molecular weight, left to right. The dotted line is the equilibrium value and the solid circles denote the crossover times from Fig. 2(a).

stretch for extended periods of time ($>\tau_I$), as seen previously in bulk simulations [18,19].

We test the prediction of Eq. (1) by reexamining the T4 relaxation in a 2 μm channel. For this case, Eq. (1) predicts a crossover extension of 5%. The equilibrium extension in a 2 μm channel was measured at 6%, greater than the crossover value. Hence, equilibrium was reached and the polymer stopped relaxing before entering regime II. This result demonstrates the effective upper bound on channel heights for which two relaxation time constants will be observed. The lower bound on channel height is set by forcing the crossover extension to be significantly less than 30% so that regime I is observable within the linear force regime. Between these two limits, the parameter space for dual-regime relaxation is of practical importance because DNA with sizes of interest (~100 kbp) will exhibit two relaxation regimes in channel heights from ~200 nm to order microns.

We now compare both sets of measured relaxation times with those from previous studies [Fig. 2(b)], in particular, the assembly of data presented in Ref. [7]. The data represented by the open squares are measured by the time correlation of the orientation angle of DNA at equilibrium [7]. All other data are measured by following the relaxation of an initially stretched chain. It is clear that τ_{II} is in very good agreement with the rotation autocorrelation data taken over a range of molecular weights and channel

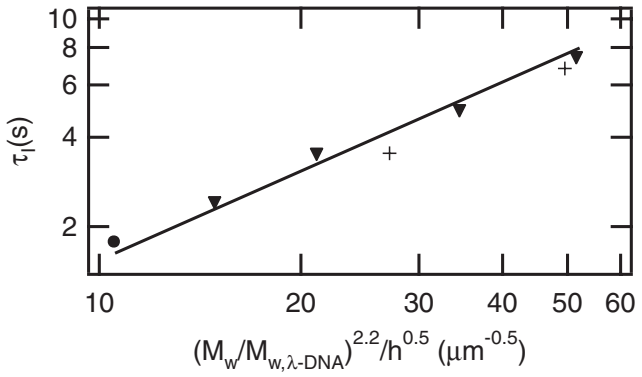

FIG. 4. Scaling results for regime I. Solid line has slope = 1. Symbols are defined in Fig. 2(b).

heights. These data were previously compared to blob theory and are well described within that framework [7]. We describe the low-extension relaxation (regime II) as arising from the steric confinement of the polymer and having the same scaling relation ($\tau_{II} \sim N^{2.45} h^{-0.92}$) as in Ref. [7].

We now turn to the regime I results presented in Fig. 2(b). τ_I is significantly less than τ_{II}, signifying that confinement effects are not as strong in this regime. Data from Bakajin *et al.*, fit at comparable extensions to those of regime I, are included on the plot and appear to follow the general trend of the regime I data. The coincidence of these two data sets may explain previous discrepancies in the literature [7]. However, a different physical mechanism is needed to explain this regime.

Using again the scaling model description of relaxation described above, the relaxation in this regime is expected to be free of the steric effects of the confining walls. Woo *et al.* [9] found that the presence of the walls does not affect the spring force law for polymers at 30% extension until the channel height approaches the persistence length. Also, Stigter was able to reproduce the data from Bakajin *et al.* by taking into account the increased drag on the polymer due to the channel walls without confinement effects on the spring force law [8]. Assuming that the spring force constant scales as in bulk ($\kappa \sim R_{g,\text{bulk}}^{-2}$), we still need a scaling for the drag on an extended polymer in slit confinement. This scaling is not available at present; however, we expect that the drag will scale linearly with molecular weight due to hydrodynamic screening [17]. Empirically, we find that a scaling of

$$\tau_I \sim \frac{\zeta}{\kappa} \sim \frac{R_{g,\text{bulk}}^2 N}{h^{0.5}} \sim \frac{N^{2.2}}{h^{0.5}} \tag{3}$$

collapses the data from this study and that of Bakajin *et al.* (Fig. 4). The drag scaling used, $\zeta \sim N h^{-0.5}$, is in agreement with previous experiments of diffusivity at equilibrium under similar confinement conditions [17]. This substitution assumes the drag on the polymer is constant throughout the relaxation process and the appearance of regime II is only due to a confinement-induced change in the spring force law.

In this Letter, we have demonstrated the existence of two separate, slow relaxation regimes present during polymer recoil in slit confinement. The existence of these two regimes has most probably been overlooked by researchers because for the same range of extensions an unconfined polymer relaxes with a single-exponential decay. While the relaxation times for these two regimes follow similar scalings with N, the scaling with h is much stronger in regime II ($\sim h^{-0.92}$) than regime I ($\sim h^{-0.5}$). Further experiments and simulations should be performed to explore in more detail this scaling dependence on h. In addition to the fundamental importance of a new relaxation mode, the existence of these two regimes has important consequences in applications such as single-molecule DNA mapping and electrophoretic separations that rely on controlling DNA conformations by the interplay of applied fields and molecular relaxation processes.

The authors thank US Genomics for funding and the microchannels used in this study. Additional funding was provided by NSF Career Grant No. CTS-0239012.

*pdoyle@mit.edu

[1] T. Squires and S. Quake, Rev. Mod. Phys. **77**, 977 (2005).
[2] P. S. Doyle *et al.*, Science **295**, 2237 (2002).
[3] E. Y. Chan *et al.*, Genetical Research **14**, 1137 (2004).
[4] N. Minc *et al.*, Anal. Chem. **76**, 3770 (2004).
[5] F. Brochard, J. Phys. (Paris) **38**, 1285 (1977).
[6] O. B. Bakajin *et al.*, Phys. Rev. Lett. **80**, 2737 (1998).
[7] C.-C. Hsieh, A. Balducci, and P. S. Doyle, Macromolecules **40**, 5196 (2007).
[8] D. Stigter, Biophys. Chem. **101–102**, 447 (2002).
[9] N. J. Woo, E. S. G. Shaqfeh, and B. Khomami, J. Rheol. (N.Y.) **48**, 281 (2004).
[10] K. Hagita, S. Koseki, and K. Takano, J. Phys. Soc. Jpn. **68**, 2144 (1999).
[11] A. Milchev and K. Binder, J. Phys. II (France) **6**, 21 (1996).
[12] T. Perkins *et al.*, Science **264**, 822 (1994).
[13] E. S. G. Shaqfeh, J. Non-Newtonian Fluid Mech. **130**, 1 (2005).
[14] See EPAPS Document No. E-PRLTAO-99-053748 for supplementary information on data analysis. Also, further images are included for aiding visualization. For more information on EPAPS, see http://www.aip.org/pubservs/epaps.html.
[15] Y. Bohbot-Raviv *et al.*, Phys. Rev. Lett. **92**, 098101 (2004).
[16] M. Daoud and P. G. de Gennes, J. Phys. (Paris) **38**, 85 (1977).
[17] A. Balducci *et al.*, Macromolecules **39**, 6273 (2006).
[18] P. Dimitrakopoulos, J. Fluid Mech. **513**, 265 (2004).
[19] P. S. Doyle *et al.*, J. Non-Newtonian Fluid Mech. **76**, 79 (1998).